

4. EXPERIMENTAL FACILITIES IN BEAM HALL

4.1 NEUTRON DETECTOR ARRAY FACILITY (NAND) & GENERAL PURPOSE SCATTERING CHAMBER (GPSC)

M. Chandra Pal, A. Kothari, P. Barua, A. Gupta, S. Venkataramanan, N. Saneesh, Mohit Kumar, K. S. Golda, A. Jhingan & P. Sugathan

During the current year, many nuclear reaction experiments have been performed using GPSC and NAND facilities. Main objective of these experiments are to study the dynamics of fission in heavy ion-induced reactions. Fission fragment (FF) mass and angular distributions have been measured and the results have been compared with statistical model predictions.

In NAND facility, major activities involved the preparation for upcoming LINAC beam experiments and some up-gradation of multi-wire proportional counters and the associated electronics. A new pair of MWPCs has been developed with some modifications in the detector housing. The new structure consists of minimum amount of aluminum in the chamber body which will reduce the scattering of neutrons. The modified detectors have been assembled and then tested offline with ^{241}Am source. The earlier set of preamplifiers were showing high frequency noise pick-up due to improper grounding. With few modifications applied to the power distribution circuit, the noise pick-up has been reduced considerably.

For tuning of LINAC beams in NAND, a beam diagnostic box (DB) has been installed in the beam line approximately 3 m before the reaction chamber. The DB is a vacuum chamber containing a target ladder with gold foil and quartz, two silicon detectors and shutters. The setup will be used for monitoring the energy and timing features of the beams before delivering to the reaction chamber in NAND. Two pneumatic shutters, movable in vertical direction, have been fixed to protect the detectors from scattered radiation when they are not in use. A view-port and CCD camera allows the view of beam on quartz.

4.1.1 Fission fragment angular distribution measurement

FF angular distributions have been measured for three reactions $^{19}\text{F}+^{182}\text{W}$, ^{187}Re and ^{193}Ir at laboratory energy range of 82-120 MeV. Fission fragments have been detected by an array of nine telescope (E- Δ E) detectors mounted inside the GPSC covering angles (θ_{lab}) $41^\circ - 170^\circ$. Each telescope consists of a gas ionization chamber (IC) followed by a silicon detector (E). Two silicon detectors mounted at $\theta_{\text{lab}} = 10^\circ$ in the horizontal plane have been used for beam monitoring and normalization. Fission fragments are unambiguously distinguished from other reaction products based on energy loss and residual energy. Extracted fission cross sections have been compared with the predictions of a statistical model calculation. The experiment has been performed by IUAC group as part of the thesis work of T. Banerjee.

4.1.2 Barrier distribution for $^{16}\text{O}+^{169}\text{Tm}$ through quasi-elastic back-scattering

The hybrid detector array in GPSC has been used in another experiment exploring the fusion barrier distribution in $^{16}\text{O}+^{169}\text{Tm}$ using quasi elastic excitation function. ^{16}O beam energy has been varied in steps of 3 MeV ranging from 17% below the barrier to 16% above the barrier. Six telescopes have been mounted at angles ranging from $+60^\circ$ to $+160^\circ$ with angular separation of 20° and other three telescopes have been kept at -110° , -122° and -134° . In addition to this, four more telescopes, each at 173° , arranged in asymmetrical cone geometry, have been used to measure the back-scattered quasi-elastic events. Two monitor detectors have been placed at $\theta_{\text{lab}} = 10^\circ$ in the horizontal plane for normalization. From the quasi-elastic excitation functions, the experimental fusion barrier distribution has been extracted. The extracted barrier distribution can be treated as a fingerprint of the reaction mechanism characterizing the importance of channel couplings. This experiment has been performed as part of a research proposal by A. Yadav et al. of IUAC.

4.1.3 Study of fusion-fission dynamics in mass 200 region

In order to examine the influence of various entrance channels on fission dynamics, FF mass distribution have been measured for $^{16}\text{O}+^{181}\text{Ta}$ and $^{19}\text{F}+^{178}\text{Hf}$, both leading to the compound nucleus ^{197}Tl . The two entrance channels lie on either side of the Businaro-Gallone critical mass asymmetry. The experiment has been carried out in GPSC using the time of flight set-up consisting of two multi-wire proportional counters (MWPC), placed at folding angles to detect the fragments. Measurements have been performed with pulsed beams of 1.0 - 1.2 ns

width around the Coulomb barrier. Time of flight and position (x and y) signals, obtained from the two detectors, have been used to extract polar and azimuthal angles of the fragments. This experiment has been performed as part of a research proposal by K. S. Golda et. al of IUAC.

4.1.4 Fission fragment mass distribution studies in Mercury region

In another experiment using the time of flight set-up, fragment mass distribution from fission of compound nuclei ^{188}Pt and ^{190}Pt , formed in the reactions $^{28}\text{Si}+^{160}\text{Gd}$ $^{12}\text{C}+^{178}\text{Hf}$ respectively, have been measured. The experiments have been performed near barrier energies to investigate the onset of asymmetric mass division in fission, as observed in beta-delayed fission of ^{180}Hg . The fission fragments have been detected using two large area MWPCs placed at about 35 cm from the target in the GPSC. The time of flight information along with the x and y positions will be used to get the mass distribution of the fission fragments. This experiment has been performed as part of a research proposal by H. Singh et al. from Kurukshetra University.

4.1.5 Measurement of mass gated neutron multiplicity in $^{19}\text{F}+^{208}\text{Pb}$

The data from an experiment, performed during NAND facility test, were analyzed to extract the neutron multiplicity gated by different masses of the fragments. Pulsed beam of ^{19}F at $E_{\text{lab}} = 110$ MeV (\square 18% above barrier) were bombarded on self-supporting targets of ^{208}Pb . The fission fragments were detected using two multi-wire proportional counters, mounted at folding angles (40° and 120° with respect to the beam direction). The energy and angular distributions of neutrons, emitted in coincidence with fission fragments, were measured via time-of-flight (TOF) method. Separation of total neutron multiplicity, into M_{pre} and M_{post} , was carried out employing the method of three moving sources, details of which can be found in Ref. [1].

The fission fragments were separated from the flux of other charged particles such as elastically scattered projectile, target recoils etc. by TOF and MWPC1-MWPC2 correlation. The mass ratio of fission fragments, $m_1/(m_1+m_2)$, were derived by velocity reconstruction method.

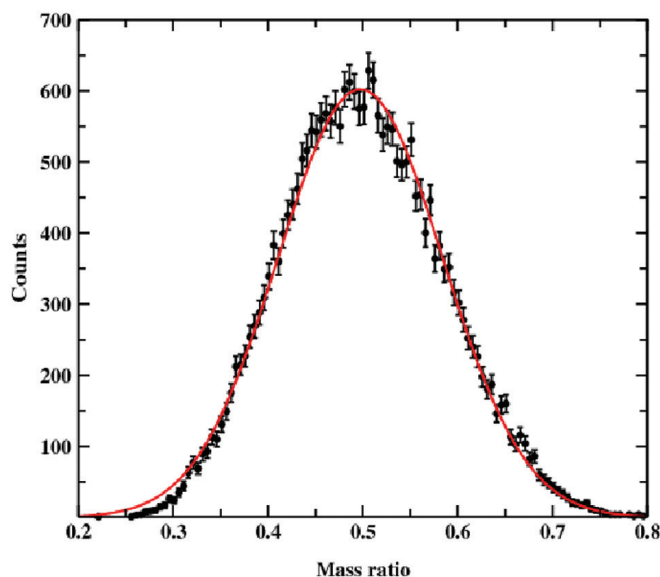


Fig.4.1.1 Mass ratio distribution of fission fragments for $^{19}\text{F}+^{208}\text{Pb}$ reaction at 110 MeV. The solid line represents Gaussian fit to data.

The neutron multiplicity was extracted for all masses and different mass gates to explore its mass dependency. For this, neutron energy spectra were gated with symmetric (0.45 to 0.55) and asymmetric (0.55 to 0.65) regions of mass ratio distribution. The value of neutron multiplicity and temperature of CN and fission fragments, extracted for singles and coincidence analysis, are given in the table.

TABLE: Extracted value of neutron multiplicity and temperature of compound nucleus and fission fragments.

Mass Gate	M_{pre}	M_{post}	T_{pre}	T_{post}
Single 3.17	1.16	1.53	0.81	
Symmetric	2.29	1.59	1.57	0.93
Asymmetric	3.44	1.05	1.57	0.76

The value of M_{pre} is found to increase in asymmetric region as compared to symmetric mass region and the correlation is similar to the one reported by Itkis *et al.* in the case of $^{18}\text{O}+^{208}\text{Pb}$ at 26 MeV excitation energy [2]. The observation was explained in terms of shell effects. As M_{pre} increases, the available excitation energy decreases which promotes shell effects and mass asymmetric fission. The preliminary analysis shows that $^{19}\text{F}+^{208}\text{Pb}$ system also exhibits shell-influenced mass asymmetric fission upon higher fission chances. A detailed analysis is in progress.

REFERENCES

- [1] N. Saneesh *et al.*, Proc. DAE Symp. Nucl. Phys. 59, 000 (2014).
- [2] M. G. Itkis *et al.*, Nucl. Phys. A 654, 870c (1999).

4.2 GAMMA DETECTOR ARRAYS (GDA & INGA)

R. K. Gurjar, Indu Bala, Kusum Rani, S. Bhattacharjee, R. Kumar, S. Muralithar and R. P. Singh

4.2.1 Experiments in INGA

INGA set-up was re-commissioned after test run with 14 Compton-suppressed Clover detectors in April 2016. The experiments with INGA started in the month of July. In August, 4 more Clover detectors with anti-Compton shields, from TIFR and UGC-DAE-CSR, were added to the set-up. During July 2016 to February 2017, about 13 experiments were successfully completed with INGA setup. To detect low energy photons, 2 LEPS detectors were also added to the set-up. The experiments were performed for lifetime measurements and gamma ray spectroscopy of nuclei from different regions of the periodic table. Most of these experiments were related to the thesis of Ph.D. students from different universities and IITs. The total beam time utilized was about 250 shifts (~2000 hours).

4.2.2 Experiments in GDA

GDA HPGe detectors were used for incomplete fusion studies for two experiments. The detectors were used for offline counting in the GDA electronics cabin. The aim of these studies was to understand the effects of structure of the reaction partners and the entrance channel mass asymmetry on incomplete fusion dynamics.

4.2.3 Technical developments

Pre-amplifier cards for Clover detectors

Pre-amplifiers of Clover detectors are very crucial for good resolution of the detectors. These are very sensitive equipment and hence also susceptible to damage. With help from the electronics group, pre-amplifier cards could be developed at IUAC. The initial performance test of these cards has been completed. The energy resolution with these pre-amplifier cards was found to be about 2 keV for gamma rays of energy ~ 1 MeV. The cards are now being tested for long time stability.

Controller for LN₂ filling

A new LN₂ controller is being designed for auto-filling of Clover detectors. This controller will be installed for the second LN₂ post for filling of detectors at the focal plane of mass spectrometer HYRA. Some of the old LN₂ manifolds have been replaced with new ones. The new manifolds have minimum 'O' ring couplings and this would reduce loss of LN₂ and frequent replacements of 'O' rings.

Servicing the Clover detectors

Four Clover detectors were successfully serviced (annealing, evacuation etc.) in the clean room designated for this purpose. One service station was also made to be able to anneal and out-gas two Clovers simultaneously. Mounting of a new FET for one of the Clover detectors is shown in Fig. 4.2.1.

Electronics and Data acquisition system

Earthing of 19" racks, housing the power supplies for ACS and Clover detectors, was completed. The racks were sorted and connected to a separate clean ground. The data acquisition and LN₂ filling control softwares were backed on a new laptop to enable any emergency backup of these softwares.

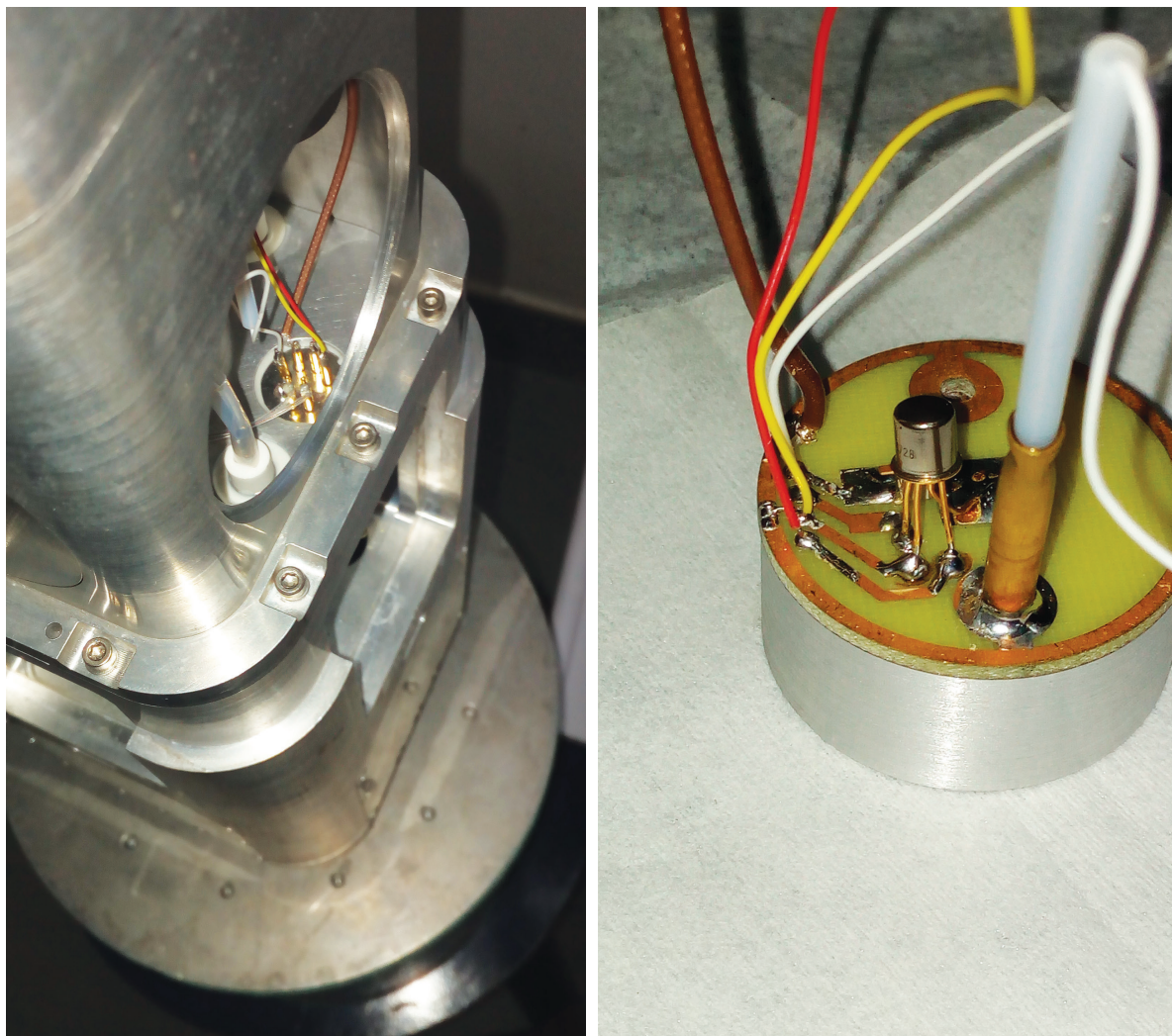


Fig. 4.2.1 (a) Clover housing opened for FET change. (b) New FET mounted.

4.2.4 Data analysis

Data from the earlier experiments were analyzed for study of high spin structure of ⁶⁶Ga and ⁶⁶Zn nuclei. In ⁶⁶Ga nucleus, 17 new transitions and several new states were identified. Theoretical calculations were also performed to understand the observed bands and the results were published. Analysis of ⁶⁶Zn is underway and was presented in the national symposium on nuclear physics. Cube analysis of high fold gamma data from our recent experiment on ¹⁰³Pd is also in progress.

4.2.5 Charge particle detector array

R. Kumar, Arti Gupta, T. Varughese, V. R. Sharma and S. Venkataramanan

Testing of front-end electronics for the upcoming charge particle detector array (CPDA) was carried out. Four CsI(Tl) detectors, supplied by the SCIONIX HOLLAND, were tested using ¹³⁷Cs and ⁶⁰Co sources. The scintillation material has a thickness of 3 mm with an active area 20 mm × 20 mm, coupled to a Si-PIN photodiode S3590-08. The sides of the crystal and the light guide were wrapped with thick white Teflon tape so that no light could escape, increasing the light collection efficiency. Front face of the crystal was covered with aluminized mylar of 2 μm (0.29 mg/cm²) to ensure uniform light collection. The detector was biased with - 30V.

Ballistic deficit method was realized by comparing the output of two shaping circuits having different shaping constants (long = 3 μ s and short = 1 μ s).

The signals from 4 crystals were measured using electronics, developed in-house (pre-amplifier and high gain stage with differential output). To avoid noise, the system was covered with black paper to provide a light-shielding as the Si photodiode could absorb any light from outside. However, the noise was mainly due to the base, which was not properly grounded, on which the detector system was placed. The circuit diagram is given below.

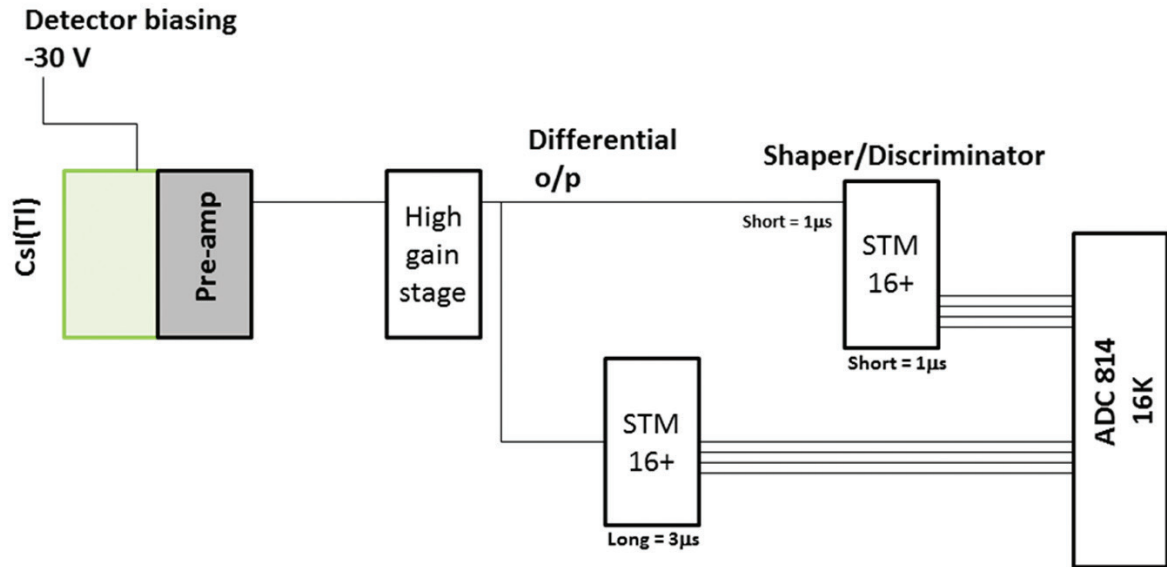


Fig. 4.2.2 Block diagram of the electronics set-up.

Resolution of < 6 % for gamma energy of 1.3 MeV (⁶⁰Co) and < 10 % for gamma energy of 662 keV (¹³⁷Cs) was obtained. Two-dimensional spectra were generated for gamma lines from ¹³⁷Cs and ⁶⁰Co sources which are shown in the figure below.

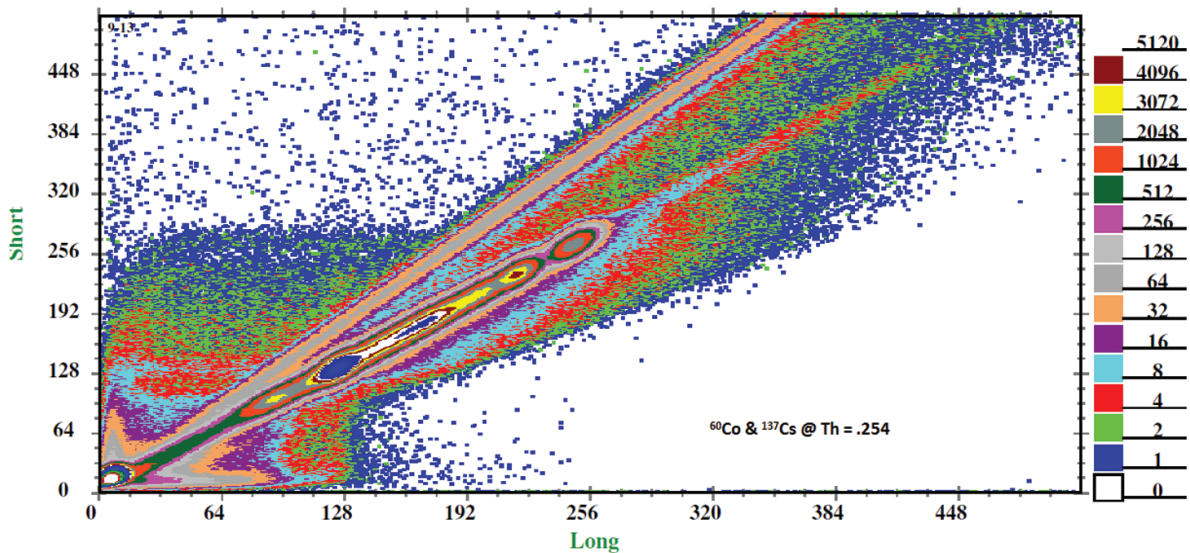


Fig. 4.2.3: Two-dimensional spectrum with ⁶⁰Co and ¹³⁷Cs sources.

After obtaining good energy resolution using the homemade pre-amplifiers and high gain electronics, the next step is to perform vacuum tests for stability.

4.3 RECOIL MASS SPECTROMETERS

4.3.1 Heavy Ion Reaction Analyzer (HIRA)

S. Nath, J. Gehlot, T. Varughese, A. Jhingan and N. Madhavan

In recent times, the floor under the shielding wall of the junction between Vault - I and Beam Hall – I was observed to have sunk in by more than an inch and this has affected the alignment of all the beam-lines. HIRA beamline and the spectrometer too required re-levelling. A detailed survey of the entire HIRA facility and beamline was undertaken right from the Switcher magnet. While the height reference points on the wall behind the Analyzer magnet (in the Vault) and that on the wall beyond HIRA (in the beam hall) were at the same level, the intermediate components downstream of Switcher magnet had gone below by varying amounts. Initially, the HIRA beamline quadrupole triplet was re-aligned. As HIRA platform rests on three points, namely, the pivot and the two wheels, it was decided to re-level the platform at these points to bring back the spectrometer components at notional beam-level. An elaborate exercise was undertaken with active role of Vacuum lab personnel. Special spacers of required dimensions, with holes and a few slots, were made so as to slip in the spacers at appropriate locations (after lifting the platform but without removing all the bolts). The HIRA platform was lifted uniformly, in a coordinated manner, with heavy-duty jacks with the crane to hold at the pivot, after disconnecting the spectrometer from the beamline components. Plumb-lines suspended at suitable positions helped to confirm that there was no side-ways movement once the operation was completed. This opportunity was used to modify the HIRA beam-line component positions and to give a face-lift to the supporting structures and cooling water-lines. The level of each HIRA component was verified with telescope and the smooth operation of HIRA rotation was established after connecting the sliding seal target chamber to the modified beamline.

Subsequently, a facility test with the beam showed that the vertical beam steerers in HIRA beamline now require negligible field. Sub-barrier fusion experiments were carried out well below the one-dimensional barrier quite easily.



Fig. 4.3.1 Re-levelling of HIRA platform

4.3.2 HYbrid Recoil mass Analyzer (HYRA)

N. Madhavan, S. Nath, J. Gehlot, T. Varughese and A. Jhingan

The experiment looking for Clustering Vs. Pairing effects of two neutrons in light nucleus ^{18}O was carried out in HYRA facility using the first stage in vacuum, momentum achromat mode. The experience gained from the facility test helped in perfecting the experimental set-up. Some crucial changes carried out in HYRA for

this experiment were the removal of the upstream beam collimator (to reduce background due to scattering), movement of the ^{27}Al target upstream to the location of gas window foil (used in gas-filled mode) to allow forward angle mounting of neutron detectors, use of target ladder in the regular target chamber with quartz (to view the beam size), gold foil (for getting time reference, intermittently) and blank frame (used during data taking), in the three positions, arrangement of six neutron detectors (three on either side) to cover forward angles from around 27° , use of momentum defining slit at the centre of Q3 split-quadrupole doublet and silicon pad detector at the focal plane (calibrated with five energy alpha source) and removal of two-thirds of spin spectrometer (TIFR) to avoid neutron attenuation. The energy and TOF of various charge states of the selected ^{16}O helped in identifying them using the scaling of (ME/q^2) ratio, the mass M being constant here. Detailed analysis of the data is in progress with preliminary results agreeing with theoretical predictions (Prof. A. K. Jain et al.).

HYRA is getting ready for carrying out students' theses experiments using beams from Pelletron + LINAC combination to measure Evaporation Residue (ER) excitation function and/or spin distributions in gas-filled mode and an experiment to look for long-lived isomers or delayed gamma ray transitions post alpha decay, in heavy nuclei. In this experiment, the same set-up used earlier for the detection of new isomer in ^{195}Bi will be used. However, this would require the sideways movement of quadrupole doublet Q6Q7 of the second stage of HYRA, on pre-installed linear rails.

For a future campaign of focal plane isomer decay measurements in weakly populated heavy nuclei, to be undertaken subsequent to HYRA-INGA campaign, more Clover detectors will be used at the focal plane of first stage of HYRA. The mechanical structure to hold the seven clover detectors has been fabricated at IUAC workshop (shown below with the final design) and a new focal plane chamber consisting of a new, compact MWPC and silicon detector will be developed.

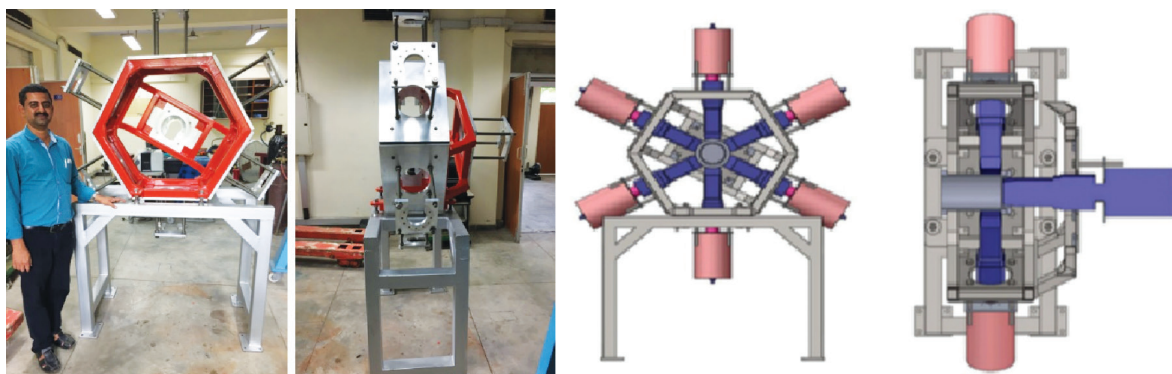


Fig. 4.3.2 Structure to mount 7 Clover HPGe detectors at HYRA focal plane and the design for the same.

4.4 MATERIALS SCIENCE FACILITY

A. Tripathi, K. Asokan, V.V. Sivakumar, Fouran Singh, S.A. Khan, P. K. Kulriya, I. Sulania, R.C. Meena

The research programmes of a large number of users from different universities and institutions continued to utilize materials science facilities. This year there were a total of 45 user experiments spread over 135 shifts and were performed without any major beam time loss due to facility break down in materials science beamline in beamhall I. BTA experiments associated with students' Ph.D. programmes continued to get priority with 17 runs spread over 53 shifts. Though the swift heavy ion (SHI) irradiation and related experiments mostly utilize irradiation chamber in the materials science beamlines in beamhall-I, 2 experiments running over 5 shifts utilizing in-situ XRD facility, were performed in the second materials science beamline in beamhall-II. Besides this, 2 experiments of 6 shifts requiring low fluence irradiation were performed in GPSC beamline. Experiments are being done in areas of SHI induced materials modification and characterization and the details are given in Section 5.2.

The materials synthesis and characterization facilities such as XRD, AFM, SEM, Raman, UV-Vis, I-V, Hall measurement etc. are heavily utilized by users. This year more than 2000 samples were characterized.

4.4.1 Maintenance of Irradiation chambers in Beam Hall I

S. A. Khan, R. C. Meena, A. Tripathi

The beamline was used by large number of materials science users and 41 experiments of 126 shifts were performed in this chambers.

4.4.2 Contact angle measurement setup

I. Sulania

The contact angle measurement set-up is being used by many users (with the help of Ms Chetna Tyagi) on a regular basis. The system is used to study hydrophobic or/and hydrophilic nature of the samples. An air bubble problem in system was resolved with refilling water. Nearly 115 samples from 12 users were studied using the contact angle measurement.

4.4.3 Scanning Probe Microscope

Indra Sulania, A. Tripathi

The Atomic Force Microscopy facility ran satisfactorily throughout last year without any major problem. A minor problem with the system monitor was diagnosed and rectified the same day without any disruption. About 315 samples were characterized with SPM in different modes from 54 users. These included 11 samples in MFM mode, 4 samples in C-AFM mode and about 300 samples in Tapping AFM mode.

4.4.4 Field Emission Scanning Electron Microscope (FE-SEM)

S.A. Khan, A. Tripathi

TESCAN MIRA II LMH scanning electron microscope at IUAC was utilized for characterizing various types of samples of users from 33 different institutes/universities. This microscopy was performed for 110 users this year to study surface morphology of 602 samples and compositional analysis of 302 samples in energy dispersive x-ray spectroscopy mode. The electron emitter of FESEM was replaced with a new electron emitter (Denka TFE) in February 2017. The new emitter was installed and tested by the authorized Indian engineers of TESCAN BRNO.

Quorum Technologies Q150TS sputter coater is utilized to coat the samples with conductive coating to eliminate the charging effect on electron incidence. This year, the coater was used to deposit Au-Pd thin film on 315 such samples of 46 users.

4.4.5 Status report on spectroscopy facilities

Pawan K. Kulriya and Fouran Singh

There have been several experiments besides regular upkeep and utilization of the structure and spectroscopy facilities for research in materials science. There is no implementation of any new facility. However, In-situ x-ray diffraction (XRD) facility has been extensively used for structural characterization of materials in the two modes namely, (a) off-line XRD (temperature varying from 20 K to 300 K) of the pristine and post irradiated sample, and (b) *in-situ* XRD for the investigation of swift heavy ion induced structural phase transformation. This year offline XRD system has been used for characterization of around 365 and 100 samples in the GIXRD and Bragg-Brentano geometry, respectively. Four *in-situ* experiments, in which structural characterization was carried out during ion irradiation, were also performed. A study related to temperature dependent irradiation induced structural transformation on the BaTiO₃ was carried out by irradiating it at different temperature (20K and 300 K), is published as "Phase dependent radiation resistant behaviour of BaTiO₃: An *in-situ* X-ray diffraction study, R Kumari, P. K. Kulriya *et al.*, Journal of the American Ceramic Society 2017. However, this year, low temperature XRD experiments couldn't be performed due to leakage of helium gas from the cryostat. Another facility namely high temperature irradiation setup also exists in the same beam line. Two experiments were performed by keeping target at elevated temperature during swift heavy ion irradiation.

Micro-Raman facility is another heavily utilized facility for the materials characterizations. This facility operates in two modes as *ex-situ* and *in-situ* modes. About 1200 spectra were measured for large number of users across the country in *ex-situ* mode. This year three runs of *in-situ* micro-Raman measurements during irradiations were also successfully conducted. Facility is operational and being utilized regularly. However, laser power has

gone down and thus new laser may be procured in future. The other facilities such as UV-photoluminescence, ionoluminescence and UV-Vis-NIR are also operational and being utilized for regular experiments and about 210, 154 and 70 spectra were measured on various types of pre- and post irradiation samples. Implementation of new FTIR facility is under process. Solar simulator facility for the characterizations of solar cell and photo diodes were also implemented in the last few years under SERB funded project. This facility is in regular operation and has been utilized for about 90 measurements. Though there are series of good publications based on the utilization of these facilities which emerged during this period; few highlights of works are reported in the results section 5.2.

4.4.6 Thermal evaporation and rf parallel plate diode sputtering systems

V. V. Siva Kumar

The RF parallel plate diode sputtering set-up was maintained in proper working condition. The base vacuum of the system was improved to 8.6×10^{-7} torr. A shutter was incorporated between the anode and cathode. It was attached to the top plate of the deposition chamber using an MDC rotatable feed through.

The RF sputtering set-up was used to deposit thin films using ZnO, SnO₂, TiO₂-SnO₂, SnO₂-ZnO, SnO₂-TiO₂-ZnO targets. The substrate temperatures used were from room temperature to 600 °C. A total of 90 thin films were grown for users for their ion beam studies. Thin films of ZnO and ZnO-Ag were also grown, by rf sputtering, for structural and optical studies.

The ball milling system was used to pulverize thermo-luminescent materials for using them for ion beam related studies. Users from University of Baroda and Delhi University used the system for their research work.

4.4.7 A.C. Susceptibility Measurement Set-up

Ramcharan Meena, K.Asokan, A.K. Rastogi

Magnetic susceptibility measurements are indispensable for characterization of magnetic and superconducting materials. Recently, we have fabricated an experimental set up for the precise measurements of small quantities (less than 200 mg) of samples between 10-300 K temperatures. This set-up has the following features:

- Measurement from 10-300 K, and rapid change of samples.
- High sensitivity: detection of less than one mg of superconducting or ferromagnetic inclusions in materials.
- Calibrated for obtaining absolute values of ac-susceptibility $\chi_{a.c}$ of samples.
- Minimizing the **effects of eddy current** generated in the metallic surrounding of the cryostat and correcting the effects on the signal from the samples at higher frequencies of measurement and at low temperatures
- Measurements of in-phase and quadrature component of $\chi_{a.c}$.

A.C. susceptibility $\chi = \frac{dM}{dH}$ is sensitive to the slope of M (H) and not to the absolute value. Here small changes in magnetization with field can be detected even when the moments are small. Moreover, a.c. susceptibility measurement yields two quantities: the magnitude of the susceptibility, χ , and the phase shift ϕ of magnetization to the applied field. Alternately, one can think of the susceptibility as having an in-phase, or real, component χ' and an out-of-phase, or imaginary, component χ'' . The two representations are related by,

$$\begin{aligned} \chi' &= \chi \cos \varphi \\ \chi'' &= \chi \sin \varphi \end{aligned} \Leftrightarrow \begin{aligned} \chi &= \sqrt{\chi'^2 + \chi''^2} \\ \varphi &= \arctan(\chi''/\chi') \end{aligned}$$

The imaginary component, χ'' , indicates dissipative processes in the sample. In conductive samples, the dissipation is due to eddy currents. Relaxation and irreversibility in spin-glasses give rise to a nonzero χ'' .

Secondary Coil: It is made of Delrin™ (an engineering thermoplastic from DuPont). Both sections of coil have about 2500 turns of Cu wire of 36 AWG each. The resistance of each coil is $\sim 150 \Omega$. The space in a coil can accommodate a cylindrical sample (solid/powder) of maximum diameter of 6 mm and 10 mm length; the centering error about 1 mm for this length within the coil of 15 mm length will entail uncertainty of about 5% in the measured value of susceptibility.

Primary Coil: The field coil is mounted directly on the cryostat tail of stainless tube of size of diameter ext/int equal to 32mm/29mm. The coil consists of Cu wire of 26AWG with 800 turns in 8 layers over its length of 120 mm. We have used varnish (Dr. Beck) for the impregnation of the coil. The DC resistance of the coil is 33Ω and the inductor value is 40 mH. The coil gives $\sim 0.8 \text{ Oe} / 10\text{mA}$ of current at its centre. The finite length of the coil would give a non-uniform field at the sample. We have not made any corrections for the non uniformity of the field by winding extra turns of coils at the extremity of this coil. Therefore, for this simple arrangement the non uniformity of the magnetic field is about 3% over 10mm length of the sample used.

Measurement procedure: The apparatus is used to measure samples of maximum size of 6 mm diameter and 10 mm length. In order to avoid any significant corrections related to eddy current shielding, we use frequencies lower than 100Hz. In our setup sample is mounted in a hollow plastic straw (soft drink straw) of 6 mm diameter, which can be inserted in the secondary coil assembly from the top of the cryostat through a vacuum sealing. The schematic diagram of this setup is shown in figure 4.4.1, where both the coils and all the instruments are interfaced with the computer.

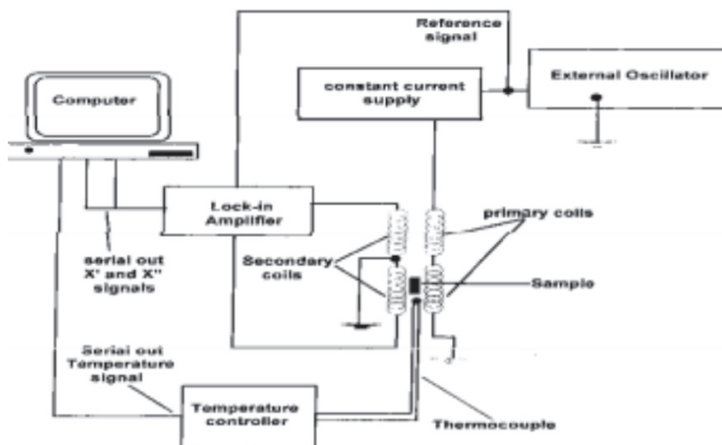


Fig.4.4.1 Schematic diagram of A.C. susceptibility measurement setup

Testing and Calibration:

Superconducting Transition: Superconducting transition behavior of high temperature superconductor was measured namely $\text{YBa}_2\text{Cu}_3\text{O}_{6.9}$, with $T_S = 90 \text{ K}$. The sample was in small pieces. The effective volume of the sample was 10^{-2} cm^3 . The current in the primary coil was 10 mA, $f = 70\text{Hz}$. For the empty coil voltages V_0 , a separate run covering the same temperature region as with the sample was performed. The subtracted voltage of the two runs $V_S - V_0$ is plotted in figure 4.4.2. The flux expulsion from the volume of a superconductor ($\chi = -1/4\pi$ in CGS, $-1/\mu_0$ in SI unit) can be used to calibrate the apparatus for absolute value of magnetic susceptibility.

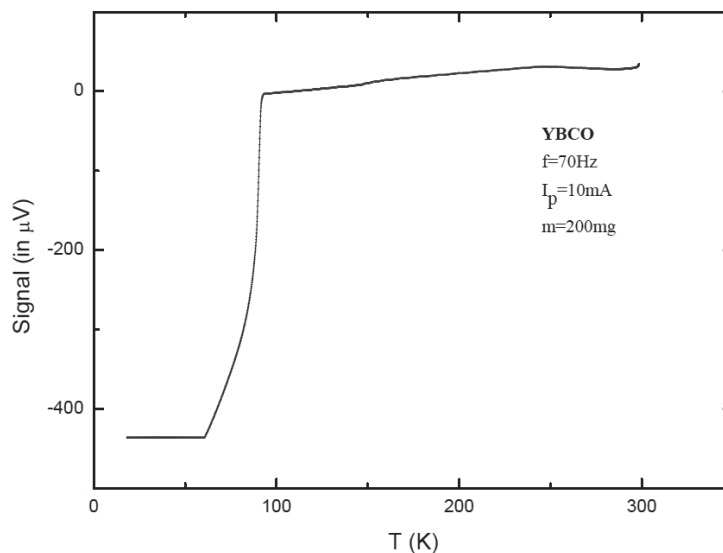


Fig.4.4.2 Superconducting transition of $\text{YBa}_2\text{Cu}_3\text{O}_{7-x}$

Curie Law Behaviour: Paramagnetic materials showing Curie-law were characterized from 10-300 K. Here a plot between inverse of signal ($V_S - V_0$) and temperature gives straight line. The measurements served to test, i) the quality of the temperature measurement and ii) linearity of the voltage signal throughout the temperature range. In addition to this, there may be changes in the reference voltage (of magnetic field) that is used to measure the in-phase component of the magnetic signal via Phase Sensitive Detector.

Paramagnetic samples, viz. Dy_2O_3 and $\text{FeSO}_4 \cdot 7\text{H}_2\text{O}$ were characterized with the set up. For paramagnets above $T > |\theta|$, $\chi_{a.c.} = \frac{C}{T - \theta}$, here C = Curie constant $C = [(\mu_{\text{eff}}/\mu_B)^2]/8 \text{ cm}^3\text{-K-mole}^{-1}$ and θ = Weiss temperature.

In case of $\text{FeSO}_4 \cdot 7\text{H}_2\text{O}$ [$C = 3.4 \text{ cm}^3\text{-K-mol}^{-1}$ and $\theta = -1 \text{ K}$] we used $m = 300 \text{ mg}$. The mass of Dy_2O_3 [with $C = 2[(10.82)^2] / 8$ i.e. $29.3 \text{ cm}^3\text{-K-mole}^{-1}$ and $\theta = -15 \text{ K}$] used was $m = 300 \text{ mg}$. Notice that for Iron sulphate, Curie law is valid to very low temperatures, whereas Dy_2O_3 has large χ_c and can be used for this purpose only above 25 K.

The measurements were made by using $\tilde{I} = 10 \text{ mA rms}$ and $f=70 \text{ Hz}$. We have plotted the results of our measurement after properly subtracting the empty coil voltages in figures 4.4.3 and 4.4.4. Our results are satisfactory considering that around room temperature the signals become very weak and much better results could be obtained in the set up by increasing the primary current ten folds and by doubling the quantity of samples.

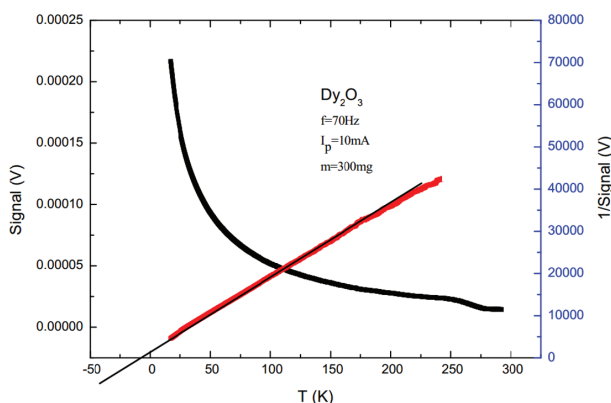


Fig.4.4.3: Signal and inverse signal showing the validity of Curie law in Dy_2O_3 .

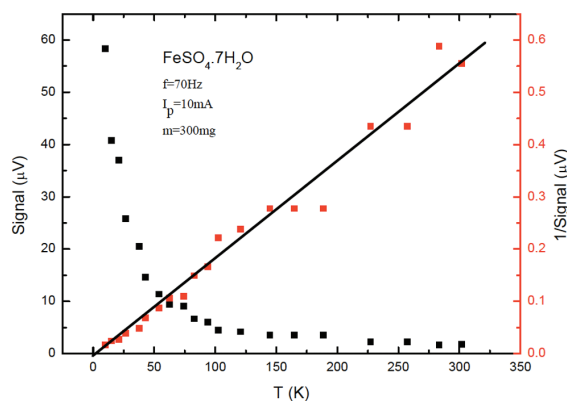


Fig.4.4.4: The output voltage relating to magnetic susceptibility behavior of $\text{FeSO}_4 \cdot 7\text{H}_2\text{O}$ plotted to show the validity of Curie law.

4.5 RADIATION BIOLOGY EXPERIMENTAL FACILITY

A. Sarma

Presently, the Banaras Hindu University and Kalyani University are continuing with the experiments related to the approved projects using the dedicated Radiation Biology Beam line of IUAC and utilizing the **ASPIRE** [Automated Sample Positioning and Irradiation system for Radiation biology Experiments] system where irradiations of cells can be done with a set of preset doses. The system is characterized by the dose uniformity over a field of 40 mm diameter within 2 % standard deviation. The mean fluence is within 1 % of the electronically measured value at the centre of the field. The characterization of the system has also been done using irradiating SSNTD [CN 85].

The radiation biology laboratory is having the following equipment to facilitate the sample preparation and post irradiation treatments.

- Two CO_2 incubators, Two bio-safety cabinets, one small laminar flow bench for cell culture
- Field Inversion Gel electrophoresis, Normal gel electrophoresis, protein gel electrophoresis set up
- Image based cell counter Countess [Invitrogen] which also gives information about cell viability and Beckman-Coulter Z2 cell counter
- PCR machine, a crude gel documentation system, UV-Vis Spectrophotometer and a Fluorescence microscope.
- Perkin Elmer Multimode Plate Reader, Eppendorf and Plastocraft Refrigerated Centrifuge and a Biotek micro-plate washer.

Apart from that, LN_2 dewars, $-80 \text{ }^\circ\text{C}$ ultra freezer, $-20 \text{ }^\circ\text{C}$ deep freezer and other refrigerators serve as the storage facilities.

The laboratory section has independent Split AC supply isolated from the central AC system. The CO_2 supply to the twin incubators is done from outside the lab area, which facilitates the replacement of empty cylinder without disturbing the laboratory environment. Regular work is going on in the laboratory on Analytical procedures involving gene expression studies using PCR, Western Blot, Fluorescence Immuno-staining studies etc. by the University Users.

4.6 ATOMIC PHYSICS FACILITY

4.6.1 A setup for studying the UV/Visible spectroscopy during ion atom collision

D. K. Swami and T. Nandi

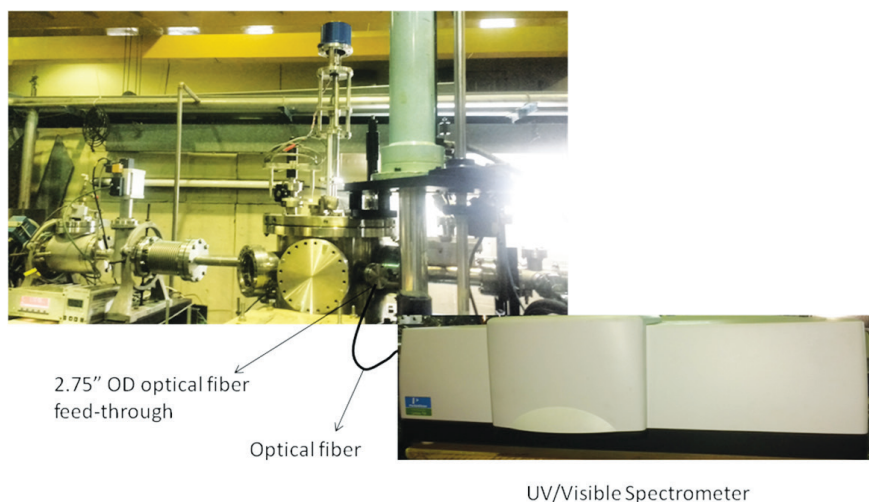


Fig. 4.6.1: UV/Vis spectrometer set up of atomic physics beam line in BH-II

A UV-Visible spectrometer has been installed for UV-Visible spectroscopy during ion-atom collisions in the General Purpose vacuum chamber in the atomic physics beam line in beam hall-2 as shown in figure 4.6.1. This spectrometer is basically a modification of the model of Perkin Elmer having a detector module covering a wavelength range of 175–3300 nm. The detector module constitutes with a photomultiplier tube (PMT) for the UV/Vis range (175-860 nm) and an indium gallium arsenide (InGaAs) and a lead sulfide (PbS) based detector combination to cover the near infra-red (NIR) range (860-3300 nm). In this spectrometer, pre-aligned tungsten-halogen and deuterium sources are used for off line testing as well as calibrations. The resolution of this spectrometer in UV/Vis and NIR range are ≤ 0.05 nm and ≤ 0.20 nm, respectively. For beam-foil UV/Visible spectroscopy, it has been coupled to the vacuum chamber with a 2.75" OD CF flange feed-through of optical fiber to transport the light from the vacuum to the spectrometer placed outside the chamber. Further, an optical focusing system is used to cut a slice of the beam-foil source to the entry of the fiber optic cable. This device can also be used to maximize the intensity in the UV/Vis spectra. In addition, the thin carbon foil target can also be moved in order to increase the intensity further.

4.6.2 Status of Multi Channel Doppler Tuned Spectroscopy

D. K. Swami, Ranjeet Karn¹ and T. Nandi

¹Dept. of Physics, Kolhan University, Chibasa-833202, India

Multi channel Doppler tuned spectrometer is a novel instrument for analyzing the x-ray emitting from fast foil excited ion beam. One such spectrometer [1] was developed in a general purpose scattering chamber of 1.5 m diameter as shown in figure 4.6.2. In the second phase, another set of the same has been incorporated so that wider angle can be scanned simultaneously. In other words, accelerator time can be used more effectively. However, it is a difficult task because of high pressure counting gas, up to ~ 1 atm required in the long 1-dimensional position sensitive proportional counters (PSPC) that is used as an x-ray detector in this setup. Following problems were encountered during a test run: (i) vacuum sealing of Mylar to the PSPC was not up the mark, (ii) gas leak causes deteriorating of beam line vacuum (iii) one gas handling system used for both the PSPCs. This time Mylar was stuck in using double sided tape instead of any vacuum sealant. A flange with small aperture of 15 mm diameter was placed in the interface of beam line and vacuum chamber was installed to isolate two sides to a certain extent. A new gas handling system with two independent gas feeding lines was installed to shut off either one in case gas leaks it. Subsequently, last year two experiments have been performed successfully. The position resolution of PSPC was found to be 700 μm at 1000 mbar pressure and 1550 V. A lifetime setup was also used in experiments. In order to have guide lines prior to high resolution studies, a low energy Germanium (LEGe) detector was also used for x-ray detection at 90° to the ion beam. The resolution of LEGe was about 300 eV at 5.9 keV with the conditions in the beam hall.



Fig.4.6.2: A setup of multi channel Doppler tuned spectroscopy

REFERENCES:

- [1] Ranjeet K. Karn, C. N. Mishra, Nissar Ahmad, S. K. Saini, C. P. Safvan, and T. Nandi, Rev. Sci. Instr. **85**, 066110 (2014).